# Electrical Properties of Conventional Polyimide Films: Effects of Chemical Structure and Water Uptake

**H. Deligöz,[1] T. Yalcinyuva,[1] S. Özgümüs,[1] S. Yildirim[2]**

[1]*Chemical Engineering Department, Faculty of Engineering, Istanbul University, 34320 Avcilar-Istanbul, Turkey*
[2]*Physics Department, Faculty of Science, Istanbul University, 34118 Vezneciler-Istanbul, Turkey*

Received 21 June 2005; accepted 8 September 2005
DOI 10.1002/app.23174
Published online in Wiley InterScience (www.interscience.wiley.com).

**ABSTRACT:** A series of conventional polyimide (CPI) films, based on pyromellitic dianhydride (PMDA) and benzophenonetetracarboxylicdianhydride (BTDA), were prepared by a two step process, and their dielectrical constant, dielectrical loss, and DC conduction behaviors were studied at different frequencies and voltages. Their dielectrical breakdown voltage, water uptake, and solubility properties were also investigated. The effects of chemical structure and water uptake on the electrical properties of the films are discussed in detail. The dielectric constants of the CPI films vary between 2.93 and 3.72 at 1 MHz frequency and they are in the following decreasing order: BTDA-DDS > BTDA-DDE > PMDA-DDS > PMDA-DDE. The structure and thermal and oxidative stability of films were analyzed by FTIR-ATR and TGA, respectively. The results showed that all CPI films have good insulating properties, such as high dielectric breakdown voltage, low dielectric constant with stability for long period of frequency, and low leakage density. Our results concerning electrical properties also suggest that electron hopping is responsible for AC conduction and Poole-Frenkel mechanism is predominant for DC conduction of all CPI films. © 2006 Wiley Periodicals, Inc. J Appl Polym Sci 100: 810–818, 2006

**Key words:** AC and DC conductivity; dielectric properties; polyimides; thin films

## INTRODUCTION

Aromatic polyimides constitute a class of high performance polymers that have excellent thermal, electrical, and mechanical properties. One of the most important applications of polyimide thin films is their use as insulators within ultra large scale integrated circuit because of their good surface planarazation characteristics, low film stress, high electrical breakdown voltage, and lower dielectric constant (less than 3.5).[1–10]

Insulating materials with dielectric constants as small as possible are preferred to achieve maximum possible device speed through smaller dimensions.[2] With increasing demand on the conventional polyimide (CPI) films with low dielectric constant, some methods have been reported, for example by Simpson and St. Clair,[11] to prepare films with lower dielectric constant.[3–5,7,9–15] One of these methods is achieved by processing large substitution groups, which is free volume in a molecular skeleton thus lowering values of both $\varepsilon_{atomic}$ and $\varepsilon_{dipolar}$.[7,9,11] Another one is the incorporation of fluorine atoms into the molecular structure of the polyimide. Hougham et al.,[12,13] Onah et al.,[14] and Park et al.[15] were mainly interested in fluorine introduction to polyimide structure to decrease the dielectric constant, which can be attributed to changes in hydrphobicity, free volume, and total polarizability.[16] The additions of pendant and bulky groups, flexible bridging units, which limit chain packing density, have all been used to increase the free volume.

Materials having dielectric constants less than 4.0 (the value of the standard $SiO_2$ insulator) have been recognized by the electronic industry as being superior in electrical performance to ceramic materials. The $\varepsilon$ values of CPI films depend on their structure and are generally in the range of 3.0–3.8.[1,8] Organic polymeric films have received great consideration as interlayer dielectric (ILD) materials. Among polymers, CPIs were first considered as ILD materials due to their excellent properties.

In the literature, studies on the dielectric properties of CPI films in AC and DC fields are not satisfactory. Sankar et al. has reported on the preparation and characterization of CPIs and copolyimides; however, they did not deal with the electric properties of these structures.[17] Homma et al. reported on the DC and AC properties of polyimide-siloxane films.[18] There are a few works on the electrical properties of modified and CPI films. One of these has been reported by Aboelfotoh et al. on the frequency dependence of dielectric loss in BPDA-PDA films.[19–23] On the other hand, Lee et al. has investigated the dielectric properties of DDE-

*Correspondence to:* H. Deligöz (hdeligoz@istanbul.edu.tr).

based polyimide thin films based on the water uptake.[10] However, no article has been established on both the AC and DC properties of CPI films in conjunction with water uptake, chemical structure, and dielectric breakdown strength.

In this study, our aim is to investigate comparatively the AC and DC electrical properties of a series of prepared CPI films. The capacitance–frequency and the *I–V* measurement techniques were, respectively, used for the determination of AC and DC behaviors of the CPI films. The frequency dependence of dielectric constant and dielectric loss (tan $\delta$) has been investigated and the conduction mechanisms for DC and AC electrical fields have been inferred from the obtained results. Moreover, thermal and oxidative stability, chemical structure, dielectrical breakdown strength, solubility, and water uptake properties of the films were investigated.

## EXPERIMENTAL

### Materials

Pyromellitic dianhydride (PMDA, purity > 97), benzophenonetetracarboxylicdianhydride (BTDA, purity > 97), diaminodiphenylsulphone (DDS, purity > 99), and diaminodiphenyl ether (DDE, purity > 99) were received from Merck Company, Germany, and they were used without any further purification. *N*-methyl pyrolidone (NMP) was distilled over $CaH_2$ and dried over a molecular sieve (5 Å) before using.

### Reactions

Preparation of conventional poly(amic acid) (PAA)

The reaction was carried out in a 100-mL three-necked round bottomed flask equipped with a thermometer, a nitrogen inlet and outlet, and a magnetic stirrer. PAA was prepared by slowly adding dianhydride compound (PMDA or BTDA) (6 mmol) into well-stirred diamine (DDS or DDE) (6 mmol) solution in NMP solution (solid 10% (w/v)) at 30°C. The reaction was continued for 3 h under an $N_2$ atmosphere at this temperature. Four different types of PAAs were prepared in the same manner. After that, the reaction was stopped and the reaction solutions were kept in a freezer to prevent any further reaction.

Preparation of CPI films

CPI films were first casted onto clean and dry glass plates by using a doctor's blade 50-$\mu$m knife from the reaction solutions. Subsequently, the films were imidized by heating at 100°C for 1 h, at 200°C for 1 h, and at 300°C for 1 h under an $N_2$ atmosphere in a temperature-controlled oven to obtain the corresponding CPI structures. The films were donated as PMDA-DDE (CPI1), PMDA-DDS (CPI2), BTDA-DDE (CPI3), and BTDA-DDS (CPI4). After this thermal treatment, the films have been removed from the glass plates by immersing into hot water. Thus, the obtained self-standing films were dried in a vacuum oven. The reactions, the structures of all CPIs, and all the donations related with the product names are shown in Scheme 1.

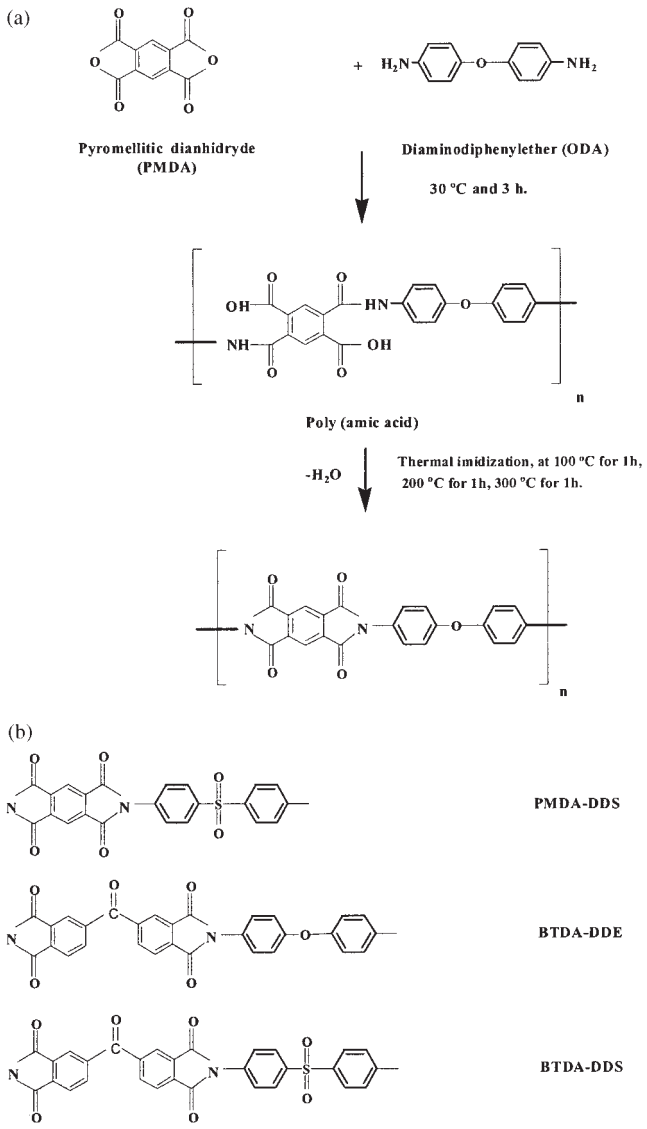


**Scheme 1** (a) Synthesis of PMDA-DDE polyimide film and (b) chemical structures of CPI films.

### Measurements

The FTIR analyses of the CPI films were carried out by a Perkin–Elmer Spectrum One with the ATR (attenuated total reflection) technique. The thermal and oxidative degradations were investigated using a Linseis L31 TGA/DTA system. The samples were heated from room temperature to 750°C under air atmo-

sphere at the heating rate of 5°C/min. The films were dried at 80°C for 10 h in a vacuum oven and weighted. After this, they were kept in a box with 55% relative humidity (RH) for 1 week and reweighted. The water uptake values of the films were calculated from the weight changes of each film. The solubility tests were carried out by immersing the films into various solvents for 1 week at room temperature.

The base and counter Au electrodes, each of 3000 Å thick, were evaporated and deposited onto the CPI films under a $10^{-5}$ Torr vacuum. In this way, Au/CPI film/Au sandwiches were ready for the measurement of dielectric properties of the CPI films. Electrical contacts were made by Indium on Au electrodes with copper wires. A sample was placed inside a chamber that isolates the sample from the outside ambient RH and room temperature.

In the dielectric and AC conduction studies, the capacitance ($C$) and the loss factor (tan $\delta$) of the CPI films were measured using a Hewlett–Packard impedance analyzer (HP4294A) in the frequency range 10 kHz–6 MHz. The capacitance was recorded at 25°C as a function of frequency. The dielectric constant was calculated from the measured capacitance data as follows:

$$\varepsilon = \frac{Cd}{\varepsilon_0 A} \tag{1}$$

where $C$ is the capacitance, $\varepsilon$ is the dielectric constant, $\varepsilon_0$ is the permittivity of the free space ($8.85 \times 10^{-12}$ MKS unit), and $d$ and $A$ are the film thickness and electrode area, respectively. The dielectric constants and the AC conductivity ($\sigma_{ac}(\omega) = \omega\varepsilon\varepsilon_0 \tan \delta$) of the CPI thin films were monitored at room temperature and at various frequencies.

In the DC conduction studies, a bias voltage in the range of 1–50 V was applied and the current flowing across the samples was measured by a Keithley 6514 System Electrometer. All of the measurements were carried out under a $10^{-2}$ Torr rotary pump vacuum at the room temperature.

The thickness of the self-standing films CPI1, CPI2, CPI3, and CPI4 was measured by means of a stylus profilometer and found to be 21, 18, 23, and 7 $\mu$m, respectively. A traveling microscope was used for the determination of the capacitor areas (~10 mm$^2$). The dielectric strength of the films was measured with an Electrotechnic Laboratorium D-7015 "Insulation Breakdown Tester" UH270, the resolution of which was 50 V for 2.5 kV and 100 V for 5 kV.

## RESULTS AND DISCUSSION

A series of CPI films were prepared by film casting and subsequently thermal imidization from the corresponding PAA solutions. The solution concentrations were chosen to be 10% (weight) to prepare good quality CPI films. The dielectric constants for the various backbone-structured CPI thin films were performed with capacitance methods at different frequencies. The films were sandwiched between gold blocking electrodes to facilitate the impedance measurements.

### FTIR spectra of the films

Structures of the films were characterized by FTIR-ATR technique and as a specimen the spectra of CPI3 and the corresponding PAA are shown comparatively in Figure 1. The peaks at 3255 and 1658 cm$^{-1}$ are attributed to the NH-bond stretching absorptions in the PAA structure, obtained by the reaction of BTDA-DDE. The peak at 3255 cm$^{-1}$ has completely disappeared and the peak at 1658 cm$^{-1}$ has considerably decreased its intensity after thermal imidization. Furthermore, we observed all the expected imide bands at 1777, 1713 (C—O stretching), 1370 (C—N stretching), 827, and 715 cm$^{-1}$ (C—O asymmetric stretching). In addition, a peak at 1225 cm$^{-1}$ appeared due to the presence of ether linkage in DDE structure. The same peaks have been observed in the other conventional CPI films' spectra too.

### TGA of the films

Thermal and oxidative stability of all the films were analyzed by TGA/DTA technique and the curves are depicted in Figure 2 and Table I. All of the CPI films have shown medium thermal stability in air due to the presence of bending bonds of (—O—) and (—$SO_2$—) in the CPI structures. We may conclude that the thermal stability of CPI films is in the increasing order CPI4 < CPI3 < CPI2 < CPI1. Thermal degradation has occurred in a single step, starting from nearly 400°C in air. It was expected that thermal stability of CPIs can be improved with increasing rod-like structure. PMDA-based CPI films exhibited better thermal-oxidative degradation stability than the BTDA-based ones. The same result was also reported by Tamai et al.[24]

### Electrical properties of the films

#### Dielectric constant

The frequency dependence of the dielectric constant is a very important factor to be considered for dielectric materials in their microelectronic applications. The dielectric constant and dielectric loss are plotted against log $f$ in Figures 3 and 4, respectively. One can see from Table II that at 100 KHz, the dielectric constants of the CPI films vary in the 2.93–3.72 ranges depending on the chemical structure. CPI1 has the

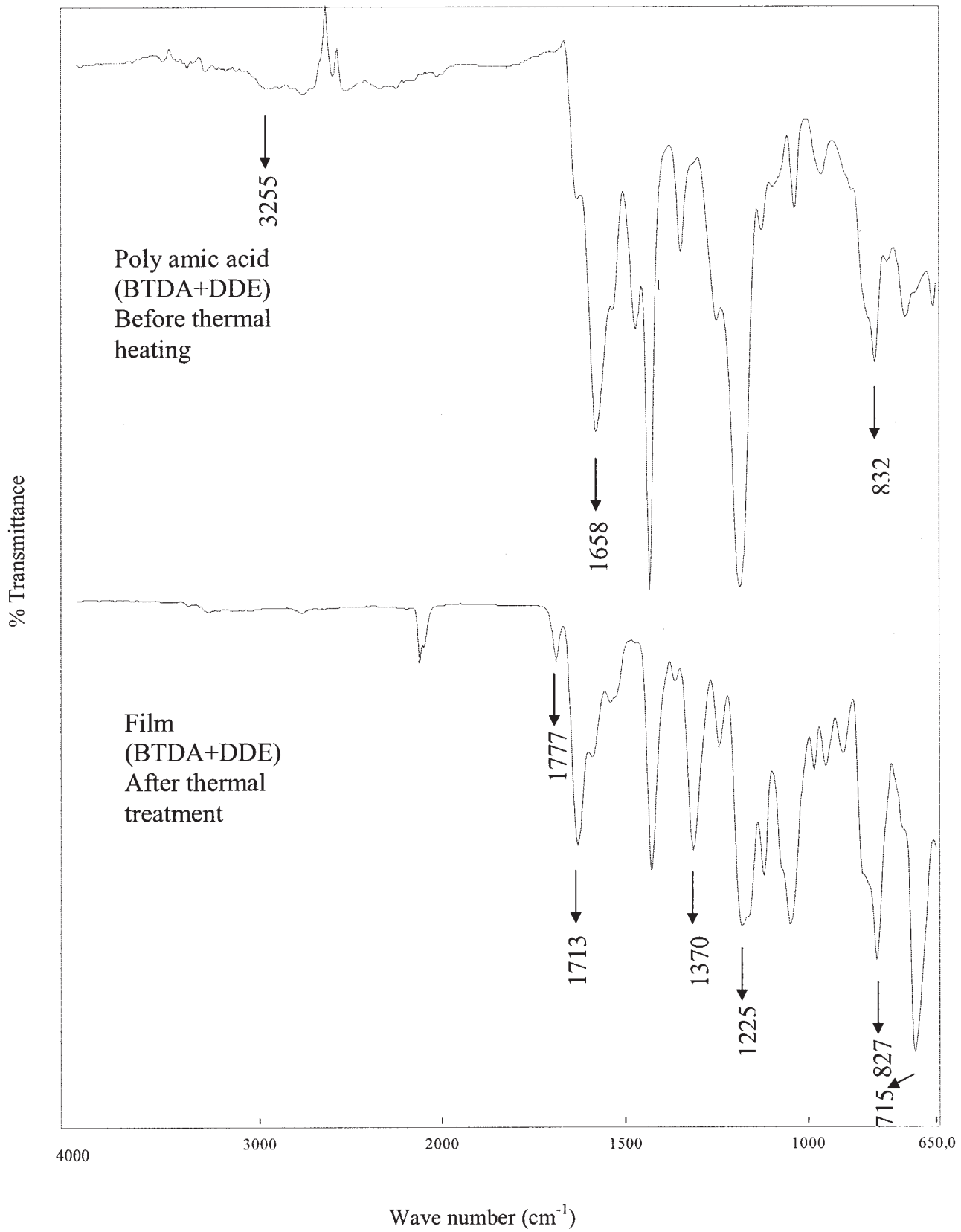


**Figure 1** FTIR spectras for (a) BTDA + DDE PAA before thermal imidization and (b) BTDA + DDE polyimide film after thermal imidization.

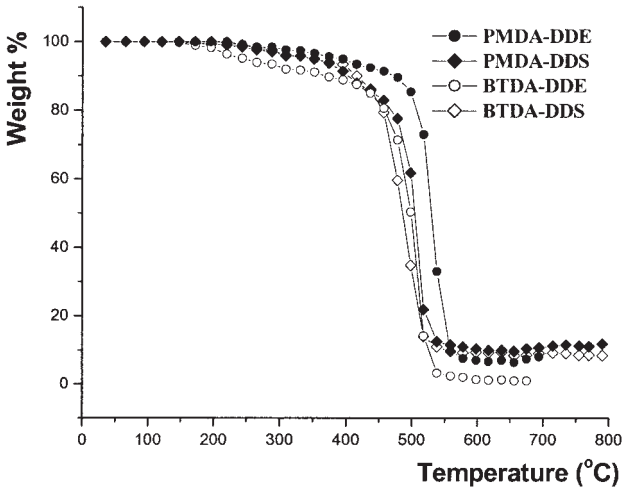


**Figure 2** TGA curves for all CPI films.

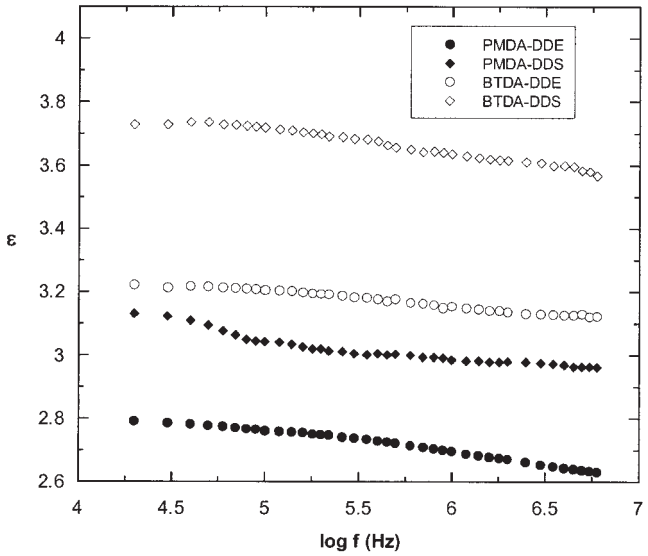


**Figure 3** Dielectric constant $\varepsilon$ versus frequency for all CPI films at room temperature.

smallest dielectric constant, while CPI4 has the largest one. Although the thickness of the films are different, we compared the dielectric constants of the all CPI films depending on the experimental fact that for films thicker than 1 $\mu$m the dielectric constant does not vary with thickness.[2] The dielectric constant of CPI thin films may be affected by decreasing the molecular packing efficiency of their chemical structures. A low molecular packing order can lead to a decrease in the number of polar group in unit volume. In other words, fewer polarizable groups in unit volume may lead to a low dielectric constant for CPI thin films.

PMDA-based films have shown more insulating properties than BTDA-based ones. It is clear that BTDA has more polarizable groups than PMDA. Furthermore, DDE-based CPI thin films have lower dielectric constants than DDS-based ones due to larger polarity of DDS. If we consider the dielectric constant of CPI3 and CPI4, it is seen that the sample CPI4 has a larger dielectric constant than the sample CPI3. This can be explained by the existence of sulfone groups in the sample CPI4. The electron density of S atoms forms extra polarization by sliding on the oxygen atoms and this causes an increase in the dipole number density. In the DDS structure, the charge distribution that slided on the oxygen atoms is two times as in the DDE structure. Therefore, the electronic conductivity of CPI4 is twice compared with that of CPI3 and the conductivity is completely realized over the $\pi$ bonds.

**TABLE I**
**Thermal and Oxidative Stability of All CPI Films**

| Film symbol | Temperature (°C) 10% weight loss | 50% weight loss | Residue[a] |
|---|---|---|---|
| CPI1 (PMDA + DDE) | 415 | 485 | 8.6 |
| CPI2 (PMDA + DDS) | 405 | 505 | 11.2 |
| CPI3 (BTDA + DDE) | 355 | 500 | 10.4 |
| CPI4 (BTDA + DDS) | 465 | 530 | 8.0 |

[a] The remaining residue at 750°C.

## Frequency dependence of dielectric constant

The dielectric constant was calculated, according to the usual parallel plate capacitor formula. From Figure 3, one can see that $\varepsilon$ slightly decreases with increasing frequency when temperature is kept constant at room

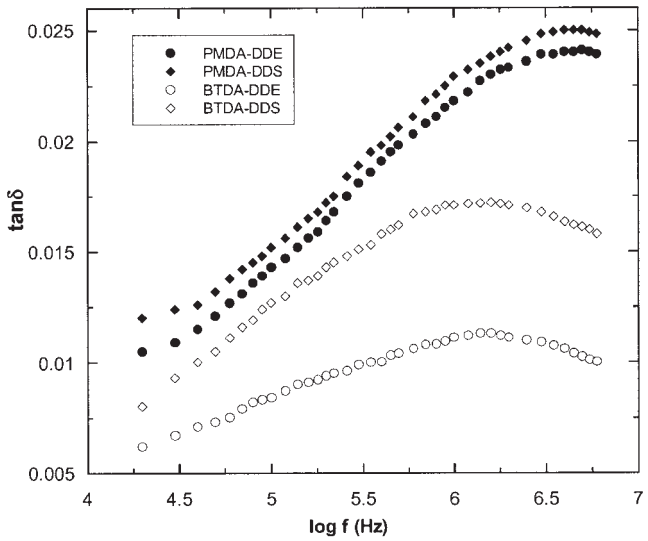


**Figure 4** Dielectric loss tan $\delta$ versus frequency for all CPI films at room temperature.

**TABLE II**
**Dielectric Constant, Dielectric Breakdown Voltage, and Water Uptake % of All CPI Films**

| Film symbol | Dielectric constant | | | Dielectric breakdown constant (kV/mm) | Water uptake (%) |
|---|---|---|---|---|---|
| | 100 kHz | 1 MHz | 10 MHz | | |
| CPI1 (PMDA + DDE) | 2.93 | 2.85 | 2.77 | 168 | 1.35 |
| CPI2 (PMDA + DDS) | 3.05 | 2.98 | 3.04 | 145 | 1.47 |
| CPI3 (BTDA + DDE) | 3.20 | 3.15 | 3.20 | 181 | 1.52 |
| CPI4 (BTDA + DDS) | 3.72 | 3.63 | 3.87 | 153 | 1.71 |

temperature. The dielectric constant of polymers is generally known to decrease gradually with increasing frequency because the response of the electronic, atomic, and dipolar polarizable units vary with frequency. This behavior can be attributed to the frequency dependence of the polarization mechanisms.[19,25] In a polymer, the magnitude of the dielectric constant is, therefore, determined by the ability of the polarizable units to orient fast enough to keep up with an applied AC electric field. When frequency increases the orientational polarization decreases, since the orientation of dipole moments need a longer time than electronic and ionic polarizations. This causes the dielectric constant to decrease. For many microelectronic applications, dielectric materials with stable dielectric constant and dissipation factor values across large frequency and temperature range are highly preferred. Our results (depicted in Figure 3) show that our samples satisfy these properties.

## Frequency dependence of dielectric loss

One can see from Figure 4 that although the dielectric loss curves of CPI1 and CPI2 follow each other, the dielectric loss curves of CPI3 and CPI4 separate from the first two and also from each other. Furthermore, the dielectric loss values of CPI1 and CPI2 are higher than the dielectric loss values of CPI3 and CPI4, and the dielectric loss curve of CPI3 is the lowest. Moreover, the peaks of the CPI3 and CPI4 are broader. The broadness of the relaxation loss peak may be illuminated due to the existence of a superposition of different dipole relaxation periods.[2,26,27] CPI4 has a broader peak compared with that of CPI3. This may be explained by the presence of larger amount of dipoles in the polymer unit and the higher water uptake property of CPI4. BTDA has higher water uptake values because it has more free volume between the molecules. Highness of the dielectric loss of samples including DDS is due to the increase of number of dipoles. The maximum of the relaxation peak of samples based on PMDA is almost twice of the higher maximum of the relaxation peak of BTDA-based samples. This is attributed to the higher rigidity of PMDA, which obstructs the motion of the included dipoles. On the contrary, the elasticity of BTDA due to C═O bonding makes the movement of dipoles easier in BTDA-based samples.

## Frequency dependence of AC conductivity

The AC conductivity of CPI films has been calculated from the measured values of the capacitance, dissipation factor, and capacitor area for each frequency at room temperature. Using the obtained data, the frequency dependence curves of AC conductivity for CPI films are shown in Figure 5. It is observed that the AC conductivity, $\sigma_{ac}(\omega)$, increases as frequency increases in all CPI films. Such a behavior can be described by

$$\sigma_{ac}(\omega) = A\omega^{S} \tag{2}$$

for several low mobility polymers and even for noncrystalline materials. Here, $\omega$ is the angular frequency, $A$ is a temperature independent constant, and $s$ is the frequency exponent, the value of which is used to understand the conduction or relaxation mechanism in insulating materials.[28] The estimated values of the exponent $s$ for CPI1, CPI2, CPI3, and CPI4 polyimide films were found as 1.11, 1.12, 1.07, and 1.09, respec-

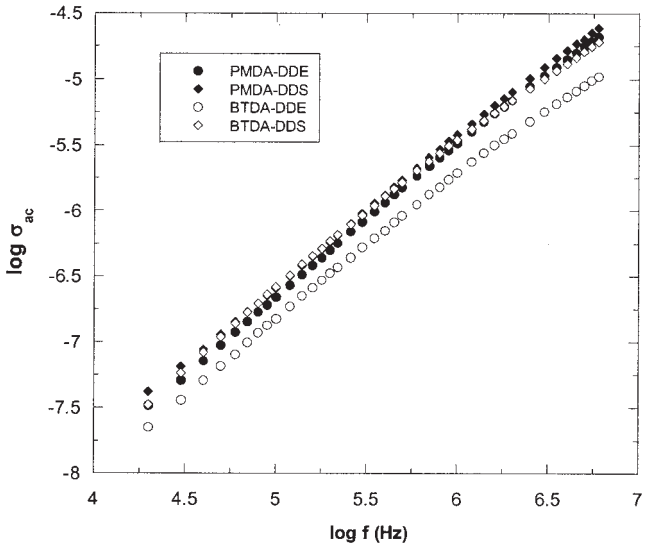


**Figure 5** Dielectric conductivity versus frequency of CPI films at room temperature.

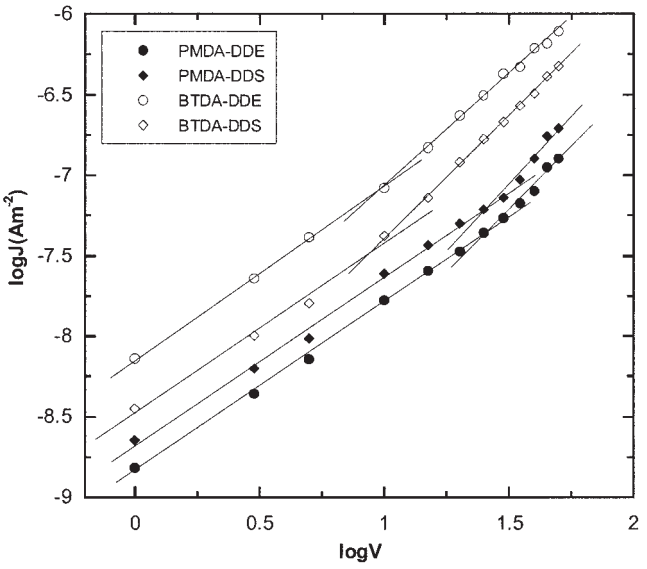


**Figure 6** Current density log $J$ versus voltage log $V$ for CPI films at room temperature.

tively, that is in the vicinity of 1. By following the previous explanations concerning the conductivity mechanisms,[28,29] we can conclude that the hopping conduction mechanism is valid for all CPI films.

## DC conduction

The variation of current as a function of the applied voltage on the CPI thin films is shown as log $J$ versus log $V$ curves in Figure 6. It is observed that the current has voltage dependence in the form $I \propto V^n$, where $n$ depends on the applied electric field and temperature. CPI3 and CPI4 exhibit ohmic conductivity properties at low fields up to 10 V and after this voltage show nonohmic behaviors, and the slopes for samples CPI3 and CPI4 in the nonohmic region have been calculated as 1.35 and 1.53, respectively. Interestingly, in contrast to the CPI3 and CPI4 samples, the CPI1 and CPI2 samples show ohmic conductivity properties up to 25 V. After 25 V, slopes for samples CPI1 and CPI2 in the nonomic region have been determined as 1.57 and 1.78, respectively. Although the current is due to thermally generated carriers in the ohmic region, a trap-related conductivity is observed in the nonohmic region. These results are in good agreement with the recently reported results.[19,30] The voltage value at which ohmic behavior changes to nonohmic behavior, the threshold voltage, is seen to depend mainly on the PMDA and BTDA structure but not on the addition of DDE and DDS. The difference in the threshold voltages (10 and 25 V) of different samples may be explained by the structural difference of the films.

There are three different types of conduction mechanisms: space charge limited conduction (SCLC), Schottky-type conduction, and Poole-Frenkel-type conduction mechanism, and one of these mechanisms will be dominant in our samples.[31] As it is seen from Figure 7, the slopes of log $J$ versus $V^{1/2}$ curves vary in the range of 1.35–1.78 in the nonohmic region. As far as we know, the SCLC mechanism is not possible in this range because in the case of SCLC mechanism, the slopes in the nonohmic region should be equal or higher than two.[32] Also, the voltage dependence of the current density in Figure 7 indicates that the possible conduction mechanisms may be either Schottky or Poole-Frenkel-type current mechanism.[33].

The Schottky-type effect is charge carrier injection to the film from the contact via the field assisted lowering of the metal insulator potential barrier. The expression for Schottky-type current density is given by

$$J = A^*T^2 \exp(\beta_S E^{1/2} - \phi_S)/k_B T \tag{3}$$

$$\beta_S = (e^3/4\pi\varepsilon\varepsilon_0)^{1/2} \tag{4}$$

where $\phi_S$ is the Schottky barrier height at the metal electrode–insulator interface in the absence of electric field, $T$ is the absolute temperature, $k_B$ is the Boltzman constant, $A^*$ is the effective Richardson constant, $E$ is the electric field that is given by $E = V/d$, where $V$ is the applied voltage and $d$ is the thickness of the sample and the constant $\beta_S$ is the Schottky field-lowering coefficient, $e$ is the electronic charge, $\varepsilon$ is the high frequency dielectric constant, and $\varepsilon_0$ is the permittivity of free space.

The Poole-Frenkel effect is the release of charge carriers from traps, lowering coulombic potential bar-

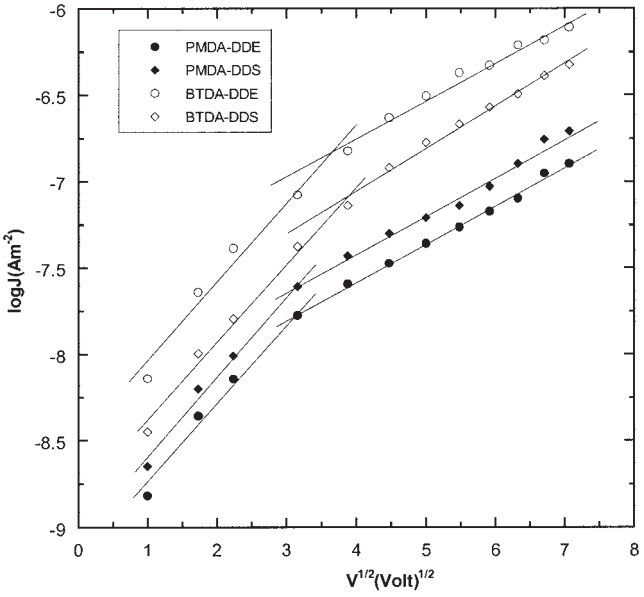


**Figure 7** Current density log $J$ versus the square root of voltage $V^{1/2}$ for CPI films at room temperature.

**TABLE III**
**Theoretical and Experimental Values of $\beta$ for All CPI Films**

| Film symbol | Experimental $\beta$ (eV $m^{1/2}$ $V^{1/2} \times 10^{-5}$) | Theoretical $\beta_s$ (eV $m^{1/2}$ $V^{-1/2} \times 10^{-5}$) | Theoretical $\beta_{PF}$ (eV $m^{1/2}$ $V^{1/2} \times 10^{-5}$) |
|---|---|---|---|
| (PMDA + DDE) | 5.86 | 2.31 | 4.62 |
| (PMDA + DDS) | 5.66 | 2.19 | 4.38 |
| (BTDA + DDE) | 5.09 | 2.13 | 4.26 |
| (BTDA + DDS) | 4.01 | 1.99 | 3.98 |

rier of a trap via the electric field. The equations for the Poole-Frenkel-type current density take the form

$$J = J_0 \exp(\beta_{PF} E^{1/2}/2kT) \quad (5)$$

$$\beta_{PF} = 2(e^3/4\pi\varepsilon\varepsilon_0)^{1/2} = 2\beta_S \quad (6)$$

where $J_0$ is the low-field current density and $\beta_{PF}$ is the Poole-Frenkel field-lowering coefficient.[34,35] A plot of log $J$ versus $V^{1/2}$ should yield a straight line if either the above mentioned two mechanisms are dominant in the four different polyimide films. Figure 7 shows the log $J$ versus $V^{1/2}$ plot for all polyimide thin films of thickness 21, 18, 13, and 7 $\mu$m. The theoretical and experimental values of the $\beta$ coefficients were calculated and compared to determine which mechanism is dominant. The experimental values of $\beta$ were obtained from the slopes of the linear portion of log $J$ versus $V^{1/2}$ plots in Figure 7 and the theoretical $\beta_S$ and $\beta_{PF}$ coefficients were calculated by using eqs. (4) and (6), respectively. The needed dielectric constant values of the four different polyimide thin films were estimated from the AC conductivity studies (Fig. 3). They have been found to be 2.69, 2.98, 3.15, and 3.63 at 1 MHz. Thus calculated $\beta_S$ and $\beta_{PF}$ values are given in Table III along with the experimentally obtained $\beta$ values. It is clear that the experimental values are closer to the calculated $\beta_{PF}$ than $\beta_S$. Hence, it can be concluded that the conduction mechanism for all CPI films is closer to the Poole-Frenkel type.

### Solubility, water uptake, and dielectric breakdown strength properties of CPI films

Solubility, dielectrical breakdown strength, and water uptake properties of the CPI films were performed. NMP, tetrahydrofurane (THF), dichloromethane ($MeCl_2$), and toluene were used as the solvents for solubility experiments. The solubility properties of the films were given in Table IV. The CPI films have shown an excellent solvent resistance in NMP, DMAc, THF, and Toluene.

Absorbed water in the package has a critical effect on the electrical properties of CPIs. As water has a very high dielectric constant, absorption in even small amounts can affect the dielectric constant of CPI films. Moreover, a structurally flexible polymer with bulky chemical groups in its structure shows more water uptake than the rigid one.[10] Water uptake properties of the CPI films are depicted in Table II. The values are in the range of 1.35–1.71. Water uptake values are in increasing order for our samples: PMDA-DDE < PMDA-DDS < BTDA-DDE < BTDA-DDS. In addition, DDE-based CPI films show lower water uptake values than DDS-based anologs.

Dielectric breakdown strengths, which is determined as the minimum value in the applied voltage at which breakdown occurs, for all of the CPI films were in the range of 145–181 KV/mm. It can be affected from the temperature changes, humidity, thickness, and purity. All results are shown in Table II. The materials to be used in microelectronics industry are highly preferred to have high dielectrical breakdown strength and low water uptake.

## CONCLUSIONS

CPI films with different combinations of monomers were prepared and the investigation was focused on their dielectric constants, thermal and oxidative stability, and electrical conduction mechanism. It is showed that PMDA-DDE has the lowest dielectric constant and dissipation factor among the prepared CPI films. PMDA-based films have shown more insulating properties than BTDA-based ones. It is clear that BTDA has the more polarizable groups than PMDA. Furthermore, DDE-based CPI thin films have lower dielectric constants than DDS-based due to the more polarity of DDS. The capacitance was found to decrease with

**TABLE IV**
**Solubility Properties of All CPI Films**

| Film symbol | Solubility | | | | | | | |
|---|---|---|---|---|---|---|---|---|
| | NMP | | THF | | $MeCl_2$ | | Toluene | |
| CPI1 (PMDA + DDE) | • | * | • | * | • | * | • | * |
| CPI2 (PMDA + DDS) | • | + | • | * | • | * | • | * |
| CPI3 (BTDA + DOE) | • | * | • | * | • | * | • | * |
| CPI4 (BTDA + DDS) | • | * | • | * | • | * | • | * |

•, insoluble at room temperature; +, soluble in hot solvent; and *, insoluble in hot solvent.

increasing frequency. It can be described by the fact that dipoles do not become oriented rapidly as fast as changing in electrical field. On the other hand, the films having higher water uptake properties showed the broader dielectric relaxation peaks. AC conductivity behavior of all CPI films obeys hopping conduction mechanism. For DC conduction mechanism, Poole-Frenkel is dominant mechanism for conducting on CPI films. Water absorption of the CPI films has decreased with lowering chain packing order.

## References


1. Ghosh, M. K.; Mittal, K. L.; Polyimides, Fundamentals and Application; Marcel Dekker: New York,1996.
2. Liang, T.; Makita, Y.; Kimura, S. Polymer 2001, 42, 4867.
3. Chern, Y. T. Macromolecules 1998, 31, 5837.
4. Chern, Y. T.; Shiue, H.-C. Macromolecules 1997, 30, 4646.
5. Chern, Y. T.; Shiue, H.-C. Macromolecules 1997, 30, 5766.
6. Meier, G. Prog Polym Sci 2001, 26, 3.
7. Fay, C. C.; St. Clair, A. K. J Appl Polym Sci 1998, 69, 2383.
8. Loke, A. L. S. Ph.D. Thesis, Stanford University, 1999.
9. Ukishima, S.; Lijima, M.; Sato, M.; Takashi, Y.; Fukada, E. Thin Solid Films 1997,308/309, 475.
10. Lee, C.; Shu, Y.; Han, H. J Polym Sci Part B: Polym Phys 2002, 40, 2190.
11. Simpson, J. O.; St. Clair, A. K. Thin Solid Film 1997, 308/309, 483.
12. Hougham, G.; Tesero, G.; Shaw, J. Macromolecules 1994, 27, 3642.
13. Hougham, G.; Tesero. G.; Viehbeck, A.; Chapple-Sokol, J. D. Macromolecules 1994, 27, 5964.
14. Onah, E. J; Oertel, U.; Froeck, C.; Kratzmuller, T.; Steinert, V.; Bayer, T.; Hartmann, L.; Haussler, L.; Lunkwitz, K. Macromol Mater Eng 2002, 287, 412.
15. Park, S.-J.; Kim, S.-H.; Jin, F.-L. J Colloid Interface Sci 2005, 282, 238.
16. Yiang, L. Y.; Ley, C. M.; Wei, K. H. Adv Mater 2002, 14, 426.
17. Sankar, C.; Hatua, K.; Maiti, S. J Appl Polym Sci 2001, 82, 976s.
18. Homma, T.; Yamaguchi, M.; Kutsuzawa, Y.; Otsuka, N. Thin Solid Films 1999, 340, 237.
19. Muruganand, S.; Narayandass, Sa. K.; Mangalaraj, D.; Vijayan, T. M. Polym Int 2001, 50, 1089.
20. Alagiriswamy, A. A; Narayan, K. S.; Raju, G. J Phys D: Applied Phys 2002, 35, 2850.
21. Sharma, B. L.; Pillai, P. K. C. Polymer 1982, 23, 17.
22. Nevin, J. H.; Summu, G. L. Microelectronics and Reliability 1981, 21, 699.
23. Aboelfotoh, M. O.; Feger, C. Phys Rev B 1993, 47, 13395.
24. Tamai, S.; Yamashita, W.; Yamaguchi, A. J Polym Sci Part A: Polym Chem 1991, 36, 1717.
25. Alegaonkar, R. S.; Mandela, A. B.; Sainker, S. R.; Bhoraskar, V. N. Nucl Instr Methods Phys Res B 2002, 194, 281.
26. Xu, G.; Gryte, C. C.; Nowic, A. S.; Li, S. Z.; Pak, S.; Greenbaum, S. G. J Appl Phys 1989, 66, 5290.
27. McCrum, N. G.; Read, R. E.; Williams, G.; Anelastic and Dielectric Effects in Polymeric Solids; Wiley: New York, 1969; p 1979.
28. Mott, N. F.; Davies, E. A. Electron Processes in Non-Crystalline Materials; Clarendon Press: Oxford, 1979.
29. Jonscher, A. K. Nature 1977, 267, 673.
30. Mathai, C. J.; Saravanan, S.; Jayalekshmi, S.; Venkitachalam, S.; Anantharaman, M. R. Mater Lett 2002, 1–5, 4145.
31. Lamb, D. R. Electrical Conduction Mechanisms in Thin Insulating Films; Methuen: London, 1967.
32. Gundlach, K. H. Phys Status Solids 1964, 4, 527.
33. Sze, S. M. Physics of Semiconductor Devices, 2nd ed.; Wiley: New York, 1981; p 254 and 402.
34. Maissel, L. I.; Gland, R. Handbook of Thin Film Technology; McGraw Hill: New York, 1970.
35. Braun, D. J Polym Sci Part B: Polym Phys 2003, 41, 2622.